EXPLICIT SIMULATIONS OF CAMBERED WEB STEERING

By

Boshen Fu[1] and James K. Good
Oklahoma State University
USA

ABSTRACT

Cambered webs are common in the web handling industry. The mechanics analyses of stressed cambered webs have been reported by several publications [1]-[3]. The majority of the test data that exist demonstrate that cambered webs steer towards their longer side. A closed form solution [4] and numerical methods [5]-[9] have been focused on the lateral behavior of the cambered web as well, but have provided no explanation of steering toward the longer side. The work that has been done focused on analyzing or modeling a cambered web span. The results from the current work demonstrate that camber in a web causes slippage between webs and rollers that produce lateral steerage. To better understand cambered web response under tension, studying the lateral mechanics of a cambered web passing over aligned rollers is the major focus of this work. Abaqus/Explicit [10] has been used to model cambered web and the transit of the web over a series of rollers. An Abaqus user defined subroutine, VUAMP, has been used to develop the first successful simulation of a web position guide interacting through contact friction with a web. This capability was needed such that a cambered web could be presented with known orientation and initial conditions to a test span where the web steering behavior resulting from camber could be studied. Simulation results are compared to experimental results [3]. The boundary conditions, which govern the steering of a cambered web in a test span, have been concluded based upon this analysis.

INTRODUCTION

As a common issue in web handling industry, cambered webs can cause steering and folding issues during web processing and converting. The mechanics analysis of stressed cambered web has been reported by several publications in last two decades, but limited success has been achieved since then. Shelton [1] and Swanson [2]-[3] tried to use beam expression to solve this problem. Swanson made three boundary condition assumptions: zero upstream lateral displacement, zero upstream slope (normal entry from the previous span), and downstream slope is equal to a constant angle that will lead the web to enter

[1] Boshen Fu works as a Modeling & Web Handling Engineer at Kimberly-Clark Corporation.

the roller normally. The 4th boundary condition is that downstream moment is a constant number which leads the downstream curvature to be equal to one over the radius of camber. The majority of the test data that exist demonstrate that cambered webs steer toward their longer side or low tension side. The experimental results suggest the friction is very important for cambered web study and multi-span models including friction effect should be taken into account for future work on cambered web [3]. Benson [4] solved the problem using a closed form solution for a cambered web span with constant radius. The zero upstream slope and displacement were implied in this work. Benson stated constant camber does not have any influence on the lateral dynamics of the web based upon analysis in [4]. However, Benson made a limited assumption: the curvature of a cambered web is a constant term in moment expression, which may oversimplify the problem. Numerical methods have been conducted to model cambered web by Jones and Olsen [5]-[9] as well, but little success has been achieved yet in this area. Meanwhile, all the work that has been done focused on analyzing or modeling a cambered web span. However, camber in a web causes slippage and steerage during processing that has yet to be involved correctly.

The analysis of steering of cambered web has been studied using different approaches, but there is no common agreement achieved. Different boundary conditions have been involved into the analysis. The most controversial one is the 4th boundary condition: the downstream curvature. Assumptions were made on the basis of zero [1] [6] or nonzero [2] constant downstream moment in different publications. However, a convincing analysis has not been done yet. Swanson in [3] also stated the 2nd boundary condition, the upstream slope of web that was usually considered as zero, might be nonzero and affects the steering of cambered web. It appears that the slope at the exit of the upstream roller in test span should be further explored in addition to the widely debated 4th boundary condition.

To better understand cambered web response under tension, studying the lateral mechanics of a cambered web passing over aligned rollers is major focus of this work. The simulation models are developed based upon experimental set-up reported in [3]. The reason to select Swanson's results is because these results are more reliable and were acquired using a better designed experimental set-up than others. Abaqus/Explicit is used to model a cambered web and the travelling process. A web guide was used in the tests to steer the camber off before the web enters the test span. To simulate this, an Abaqus user defined subroutine VUAMP is used to model a self-controlled web guide for the first time. The simulation results are compared to experimental results collected and reported in [3]. This analysis is expected to give insight with regard to kinematic and kinetic boundary conditions, if they exist or can be written simply. In this work, the experimental results are reviewed at first. Simulation results from two finite element models are compared to experimental results. The results are discussed and conclusions are drawn from this analysis.

EXPERIMENTAL RESULTS AND EARLY STUDY

In [3], the camber was cut into the web with controlled slitting knives upstream of a test section. A section with camber slit into it would be followed by a straight section. The web lateral position was maintained with a guide prior to entry to a test section. In the test section the web edge position was monitored with 5 edge sensors. The 5 sensor outputs were used to define 3rd and 4th order polynomials to continuously define the deformed shape of the web in the test section. Using these polynomials, the lateral deformations and slopes can be estimated as the web enters and exits the test span.

Analysis of cambered web response when it is moving through rollers was also discussed in [3]. As shown in Table 1, low friction means bare aluminum rollers were used in the tests and friction coefficient is considered as 0.3 typically. High friction means rollers have a silicon rubber coating (3M Company[2] 5461) which has a high friction coefficient when in contact with polyester. Tests per ASTM D1894 have shown the static friction coefficient could be 4.0 or even greater. For the low tension cases, the lateral displacements at the entry and exit to test span are all very tiny, which indicates even the lowest tension, 17.8 N, is able to pull out the camber and makes the cambered web move straight and probably enter rollers normally. On the other hand, the high friction cases do show the tension dependency: higher tension induces lower relative lateral displacements between upstream and downstream ends of the test span.

Tension (N)	Roller contact friction	Measurement at entry of test span (mm)	Measurement at exit of test span (mm)
17.8	Low	0.010	-0.028
35.6	Low	0.010	0.061
53.4	Low	0.001	0.028
17.8	High	-0.010	1.476
35.6	High	0.000	0.302
53.4	High	-0.003	0.064

Table 1 – Experimental results [3]

Conclusions have been drawn based upon measurements: cambered webs steer laterally to the low tension side (longer side) when they travel through parallel high friction coating rollers; cambered webs do not deflect laterally when low friction rollers are used; the friction coefficient between web and roller is very important, especially at the downstream roller side. All of these conclusions will be examined using Abaqus/Explicit simulations in this work. The detailed experimental setup and results are well documented in [3].

SIMULATION MODEL (1st MODEL)

Usually, similar experimental set-up should be modeled in the simulations. However, tests conducted in [3] used a complex experimental set-up. It is too time consuming to model the complete web line, which would lead to a huge finite element model. Hence, only the camber radius and test span length are kept same as experimental set-up. The roller positions and other dimensions of spans are not same as what was used in the tests. Several cases, which include different tensions and roller surface tractions, are modeled and conclusions are made based upon the analysis of simulation results.

Figure 1 shows web models and rollers set up. As shown in Figure 1 (a), the free span includes a camber, whose radius is 150 m, length is 8.89 m and thickness is 0.05 mm. The web width is 152 mm. The Young's modulus of web is 4.5 GPa and Poisson's ratio is 0.3. The roller radius is 74 mm. Figure 1 (b) indicates the details of roller set-up: the test span length between R2 and R3 is 1.52 m and there are several rollers set before the web enters R1. Two different tensions, 17.8 N and 53.4 N, which are applied on both

[2] 3M Company, 3M Corporate Headquarters, 3M Center, St. Paul, MN 55144-100, USA

ends of the web, are used in the simulations. R5 is driven with a constant angular velocity, which induces a consistent web velocity. Both tension and R5 rotation are ramped up in the first five seconds of the simulation. The total simulation time is 70 seconds. Element size is 6.35 mm × 6.35 mm. Shell elements (S4R) are used to generate the plastic web model.

(a)

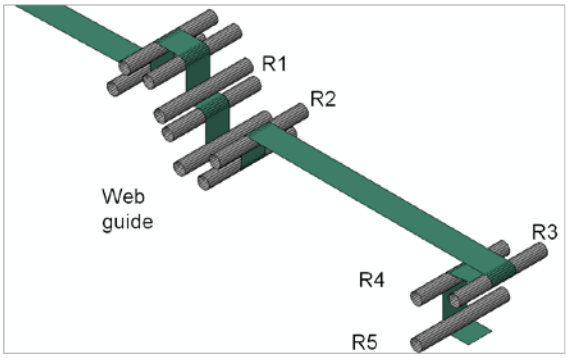

(b)

Figure 1 – Cambered web model set-up: (a) Camber in free span; (b) Roller set-up.

In the tests, a web guide was used to steer the camber off and let the web enter the test span with its centerline coinciding with a chosen zero position. It is worthy of note that the normal entry to test span might not be true in all the tests, because the entering slopes of web to the test span calculated using experimental measurements are not equal to zero in all the cases [3]. During the tests, the web guide was controlled by a web response signal which was acquired by installed edge sensors; hence it was hard to be modeled without feedback control taken into account. The approach employed in this work to model a web guide is to use an Abaqus/Explicit user defined subroutine, called VUAMP, which offers the function to model feedback control. This subroutine can be used to define the value of an amplitude function of time and to model control engineering aspects of a system when sensors are used. The "sensor" in Abaqus/Explicit modeling is not same as the real sensor. Instead, it is a node set created in Abaqus/Explicit output requests, which can return the requested value, such as, nodal displacement or nodal reaction force, to VUAMP subroutine. Each sensor value corresponds to a history output variable associated with the output database request defining sensor.

The intent of this simulation is to let the cambered web enter the test span with its centerline coinciding with a chosen zero position by controlling web guide rotation, which requires continuously steering camber by rotating the web guide smoothly when the cambered web is moving on rollers. The web guide forces the cambered web to enter the test span at a constant lateral location but does not ensure normal entry. Both the lateral position and the slope of the web have to assume steady state values as the web

enters the test section for steady state lateral behavior to be achieved in the test span. The lateral behavior of the cambered web in the test span is expected to be affected by the camber and web tension. Prior to these simulations the slope of the web entering the upstream roller of the test span was not studied either in tests or in analysis. One of the curiosities is how the slope at the entry to the test span varies through time. Therefore, the lateral deformation of the cambered web in a test span may be determined by entering slope, applied tension and contact frictional forces between web and rollers.

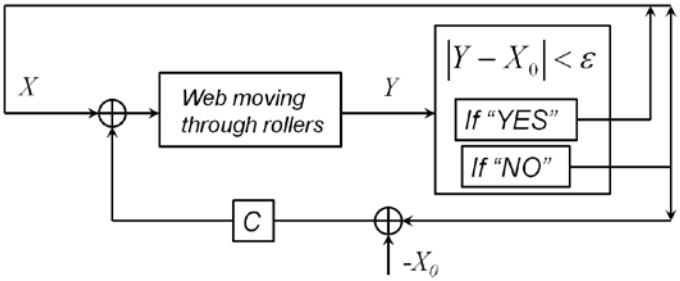

X is web guide input; Y is sensor signal; X_0 is expected web position; C is weight constant; ε is stop criterion.

Figure 2 – Flow chart of feedback control

The feedback signal for control is the error between the expected lateral coordinate and current lateral coordinate at the entry to R2. The error signal is used to determine the amplitude of a position web guide rotation which makes the web enter R2 at a target position. As shown in Figure 1 (a), nodes along the centerline of the cambered web do not locate at zero global coordinates along cross-machine direction (CMD) or Z direction. The expectation herein is to move the cambered web to zero global coordinate by applying web guide rotation. The sensor is used to obtain displacement information of a certain node. The intention is to control web guide rotation to force the nodal displacement plus the initial position of a node equal to a target value. The initial positions of the nodes along the centerline of the cambered web from the meshed model are known and the nodal displacement information is collected from simulation output using the sensor, so that all that is required is to determine the guide amplitude using position value and displacement from a certain node near the guide point to control the web guide rotation and make the node move back to zero global coordinate when it is approaching the entry to R2. To model this, sensors are created along centerline of the 8.89-m-long cambered web. There is a sensor in every 12.7 mm along centerline, which is sufficient to describe the camber shape smoothly. Sensors and output request are created using Macro file instead of manual selection, which is another benefit of the Abaqus software: conducting user defined functions using the Macro file written in Python.

When the modeled sensor in the web approaches the entry to R2, it starts to return a signal, which is the nodal lateral displacement in global coordinate. In this case, the sensor nodes are activated only when they reach the entry to R2. After they move onto R2, they will be deactivated. This means the only activated sensor that is the one moving around the entry to R2 sending back control signal, which is similar to a signal sent from edge sensors in reality. In the subroutine, the lateral displacement signal from the activated sensor plus the acquired initial position of the sensor are used to calculate the

lateral displacement error. The error is summed to amplitude value (initially set as zero) from the previous step to produce a current amplitude value to control the web guide rotation. During the simulation, the web guide rotation is fully controlled by the signal from the sensor. The flow chart of feedback control is shown in Figure 2. The weight constant *C* is selected as a small number (about 4.0e-4) to ensure stability of feedback control.

SIMULATION RESULTS FROM 1st MODEL

Lateral displacement data was recorded during test results are compared to corresponding simulation results. It is not straight forward to use lateral displacement to show results. It is because during tests the location of cambered web entering test span and lateral location of web at downstream end of test span were recorded, and the entering upstream location was considered as zero location. The lateral displacement at downstream end was calculated using downstream location subtracted upstream location. Thus this lateral displacement is not in global coordinates, but the displacements from simulations are all in global coordinates. To better present the simulation results, deformed coordinate which is equal to original coordinate plus lateral displacement, is used to show the movement of web. The deformed coordinate can be also defined as the final location (x, y, z) of a node in the global coordinates after deformation.

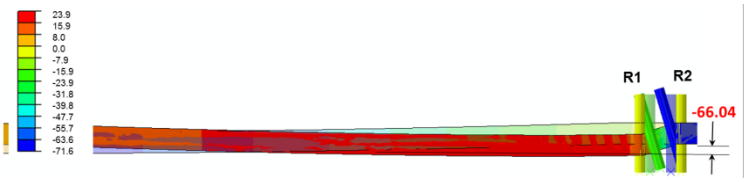

Figure 3 – Explanation of deformed coordinate

Figure 3 shows the deformed cambered web and initial cambered web (lighter color). The peak of the camber is on R2 at this time step. The original Z direction (along CMD) coordinate of peak of camber is about 66.0 mm. This means the web guide already brought the web back to zero location in global coordinate. Thus the deformed coordinate of the cambered web should be close to zero when web enters R2. Bare aluminum rollers and silicon rubber coating rollers were used in the tests which provided different friction coefficients when in contact with a polyester web. Both low and high friction coefficient cases are examined in simulations and different friction coefficient combinations are used for contact properties. Since 0.3 is typically value used for contact between bare aluminum and polymer, it is used for the contact property on each roller in the low friction coefficient simulations. The high friction coefficient is considered as 4 or even higher based on measurement. In simulations, the friction coefficient 0.3 on each roller is studied at first. Then two friction coefficient combinations, 4 and 0.1 on R3 and 0.3 for other rollers, are studied in addition to 0.3 friction coefficient case.

Study of Friction Coefficient 0.3 on Every Roller Case

The deformed coordinate at different locations are shown in Figure 4. The cambered web has really large deformed coordinate as exiting R1 which is the roller before web guide (Figure 1). After the web exits web guide, the deformed coordinates become close to zero. It can be seen in Figure 4(b) a constant nonzero entering slope is generated at R2 entry, but the entering slope at R1 entry is inconstant. From Figure 4 (a), the capability of

web guide has been proved because a large input deformed coordinate at R1 exit can be reduced to a close to zero value which also stays constant at R2 entry in the simulation. The entry slope to R2 (test span) was not measured in experiments, and the effect regarding to this slope will be discussed later.

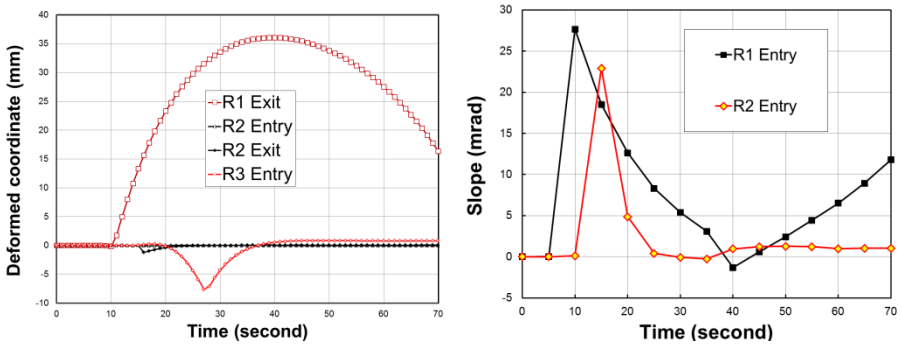

(a) (b)

Figure 4 – Deformed coordinates (a) and slopes (b) at different locations through time.

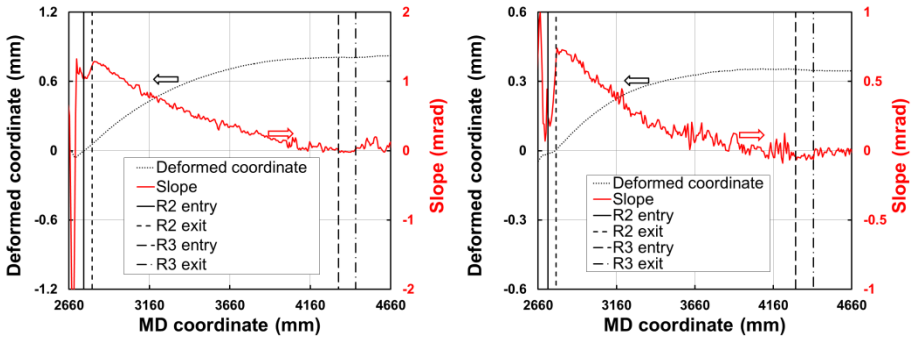

(a) (b)

Figure 5 – Lateral deformed coordinate along MD direction: (a) 17.8 N tension; (b) 53.4 N tension.

Figure 5 shows deformed CMD coordinate along centerline of web when it enters R2 and R3 under 17.8 N and 53.4 N tensions, and slopes calculated using deformed coordinates with respect to MD coordinate. Entry and exit positions of R2 and R3 are shown as vertical lines. All the curves are acquired from 70 seconds of simulations. In both plots of Figure 5, the deformed coordinates at entry and exit of R2 are all close to zero. Figure 6 shows deformed coordinate at centerline of web through time at the entries to R2 and R3 and exit of R2 in two different tension cases. The entry to R2 is where the web guide starts to steer the camber and makes the web enter R2 with an expected small deformed lateral coordinate. In Figure 6, the deformed coordinates around R2 in both cases are all small through the simulation, which indicates the web guide works nicely to steer the camber and only allows a tiny offset from zero CMD coordinate in this case. It is worthy of note that the lateral deformed coordinate of the web at the entry of R2 is

smaller than 0.025 mm, but not exact zero, which could be due to the disturbance of web guide rotation.

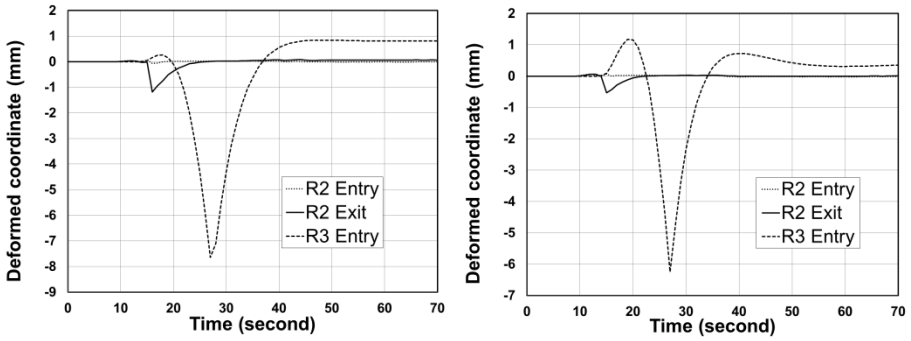

(a) (b)

Figure 6 Lateral deformed coordinate against time: (a) 17.8 N tension; (b) 53.8 N tension.

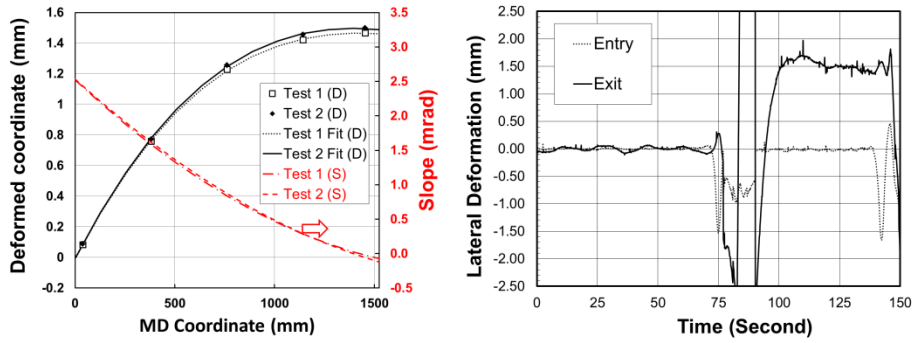

(a) (b)

Figure 7 – Experimental results under 17.8 N tension: (a) Lateral deformed coordinate along MD direction; (b) Lateral deformed coordinate through time.

The 3M test results are shown in Figure 7, which includes results under 17.8 N tension and using high friction coefficient rollers. To study the slope of cambered web in test span, the deformed coordinate curves were fitted as polynomial equations and the slopes of web could be calculated using these equations which are shown in Figure 7 (a). The curves from simulations (Figures 5 and 6) and experiments (Figure 7) have similar shape and the web is steered towards to positive direction which is the so-called longer side or lower tension side. This agrees qualitatively with the experimental results reported by Shelton [1] and Swanson [3]. The steering at downstream end does not match with each other, but the entering slopes to test span do not agree either. All the deformed coordinate results and slopes are shown in Table 2. For 17.8 N case, the entering slope from test result is twice larger than the slope from simulation result, which results in a nearly two times larger downstream steering. On the other hand, slope from test results is smaller than simulation result for 53.4 N case, and it induces a smaller downstream

steering. It appears that the nonzero entering slope of web to test span (at R2) affects downstream lateral movement significantly. As mentioned early, the exactly experimental set-up cannot be simulated with computational cost concern; hence the effect of upstream roller set-up of test span can change the entering slopes. Unfortunately, there is no data measured regarding lateral movement of cambered web in upstream span in all previous tests.

Applied tensions (N)	Simulation				Test	
	Deformed coordinate at R2 Exit (mm)	Deformed coordinate at R3 Entry (mm)	Relative displacement (mm)	Slope (mrad)	Deformed coordinate (mm)	Slope (mrad)
17.8	0.061	0.808	0.747	1.23	1.473	2.5
53.4	0.008	0.351	0.343	0.667	0.064	0.2

Table 2 – Simulations vs. Experiments

To study the 4th boundary condition, the downstream moment or curvature, moments calculated using MD stresses are shown in Figure 8. According to elementary beam theory, the Bernoulli-Euler relationship between the applied bending moment and the resulting curvature of the beam is:

$$M = EI\kappa \qquad \{1\}$$

where, E is Young's modulus which is 4.5 GPa, and I, area moment of inertia, is 1.5×10^{-8} m^4. In this cambered web case, the moment is estimated using the bending stiffness divided by the cambered radius ($1/\kappa$), which is 150 m. The theoretical moment to straighten the camber is 0.447 N·m, which is shown as horizontal double dots line in Figure 8. The moment curves in Figure 8 show neither 17.8 N nor 53.4 N case is constant in test span. In 17.8 N tension case, the moment starts as about 0.328 N·m that is much lower than theoretical value when the web exits from R2, and approaches theoretical value as the web enters R3. In the 53.4 N case, the moment starts as about 0.373 N·m and reaches theoretical value at the downstream end. The difference should be caused by the nonzero slope at the exit of R2.

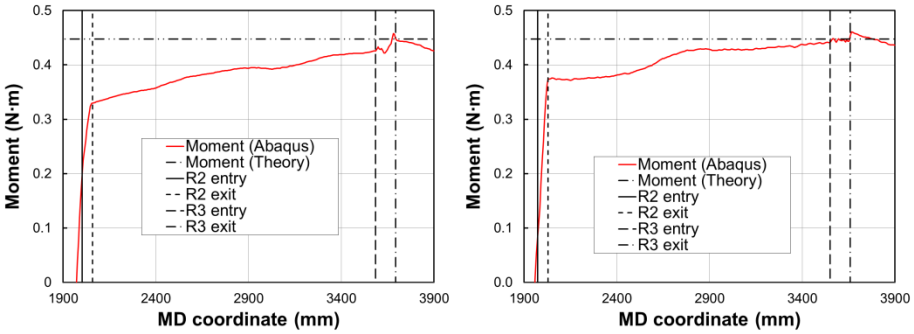

(a) (b)

Figure 8 – Calculated moments along MD direction: (a) 17.8 N tension; (b) 53.8 N tension.

Study of Different Friction Coefficients

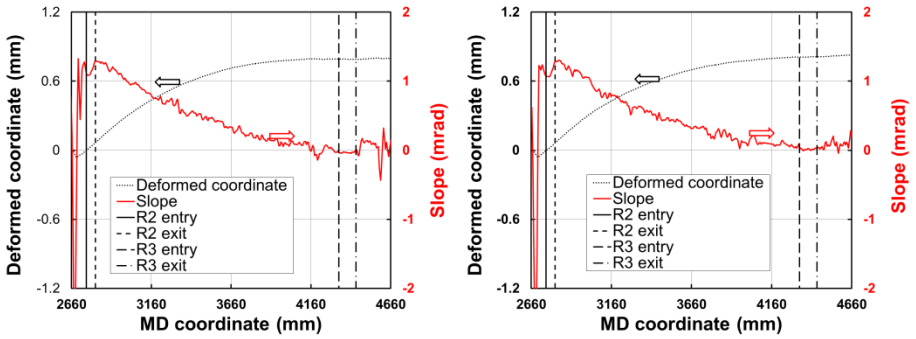

(a) (b)

Figure 9 – Lateral deformed coordinate along MD direction under 17.8 N tension: (a) Friction coefficient is 0.3 on all rollers except on R3 which is 4; (b) Friction coefficient is 0.3 on all rollers except on R3 which is 0.1.

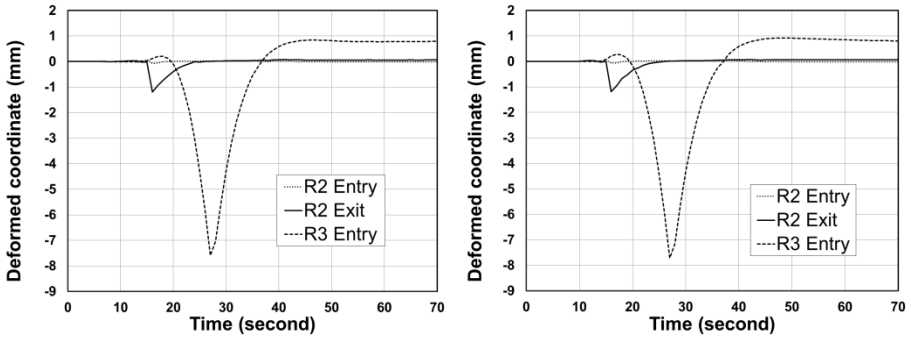

(a) (b)

Figure 10 – Deformed coordinate against time under 17.8 N tension: (a) Friction coefficient is 0.3 on all rollers except on R3 which is 4; (b) Friction coefficient is 0.3 on all rollers except on R3 which is 0.1.

Two more combinations of different friction coefficients are simulated using same model: 4 and 0.1 on R3 respectively, and 0.3 is applied on any other rollers. 17.8 N tension is used in these two cases and all other conditions are same. The intention of these two simulations is to examine the effect of different friction coefficients on downstream roller. Deformed coordinate and slope plots against MD coordinate are shown in Figure 9 for two cases. Figure 10 shows the deformed coordinate through time. Compared to Figures 5 and 6, there is no significant difference shown in these deformed coordinate plots. These results do not agree with the test results show in Table 1, which will be discussed later. The entering slopes in two cases are very close as well, and normal entry is achieved at downstream end in both cases. The calculated moments from

two cases are shown in Figure 11. The moments at upstream end are all about 0.328 N·m in both cases, which agree with the results in Figure 8 (a). But at the downstream end, the moments are slightly different: 0.433 N·m for friction coefficient 4 on R3, 0.426 N·m for 0.3 on R3 and 0.425 N·m for friction coefficient 0.1 on R3.

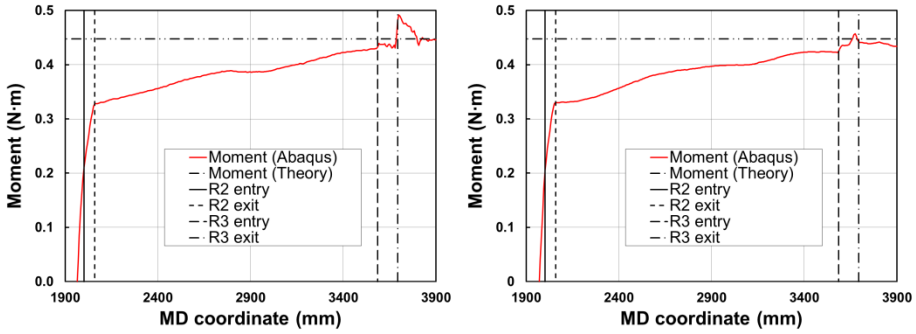

(a) (b)

Figure 11 – Calculated moments along MD direction under 17.8 N tension: (a) Friction coefficient is 0.3 on all rollers except on R3 which is 4; (b) Friction coefficient is 0.3 on all rollers except on R3 which is 0.1.

Study of Entering Slope to Test Span

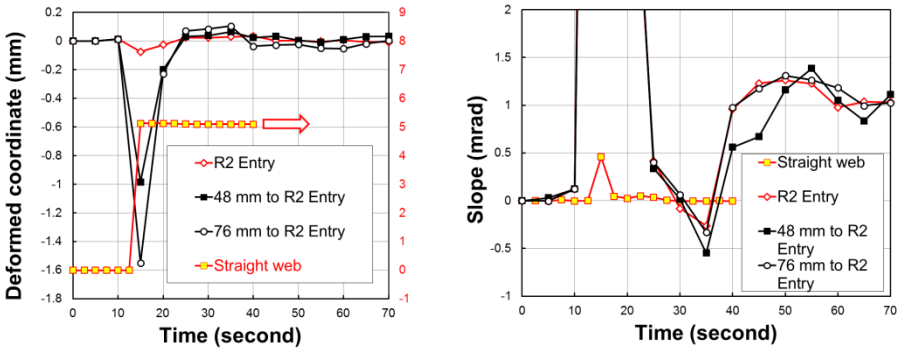

(a) (b)

Figure 12 – (a) Deformed coordinates at entry to R2 and (b) Slopes from different sensor location cases and straight web through time.

The analysis clearly leads to the argument that the slope of web as it enters testing span is a critical factor to affect the downstream steering. As shown in last two sections, similar entering slopes result in similar downstream lateral movement. The test results also indicate larger slopes induce larger downstream steering. To further explore the entering slope, different sensor locations have been examined at first: 48 mm and 76 mm from the entry to R2. The deformed coordinates are affected by sensor locations, but the entering slopes do not show significant differences as shown in Figure 12. Additionally, a straight web model has been conducted too. In this case, the web guide is used to guide

the straight web moving 5 mm laterally. The deformed coordinate curve shows 5 mm lateral movement in Figure 12 (a). The slope curve shows zero value when the straight web enters R2 in Figure 12(b). Hence the constant nonzero entering slope is dominated by the camber of web instead of the rotation of web guide.

The entering slope near R2 entry is affected by tension as well. Higher tension induces a smaller entering slope as shown in Figure 13 (b). Thus the entering slope is not affected much by the location of sensor in pre-entering span but decreases with tension increasing. Since all the rollers are aligned, the nearly constant nonzero slope of web shown in Figures 12 (b) and 13 (b) should be induced by slippage between web and roller which is a combination effect of camber of web, applied tension and web guide rotation.

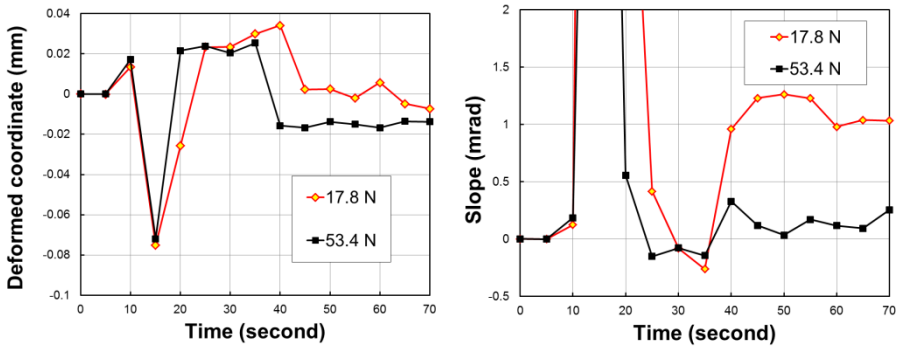

(a) (b)

Figure 13 – Tension effect: (a) Deformed coordinates at R2 entry and (b) Slopes through time.

SIMULATIONS USING A DIFFERENT MODEL SET-UP (2nd MODEL)

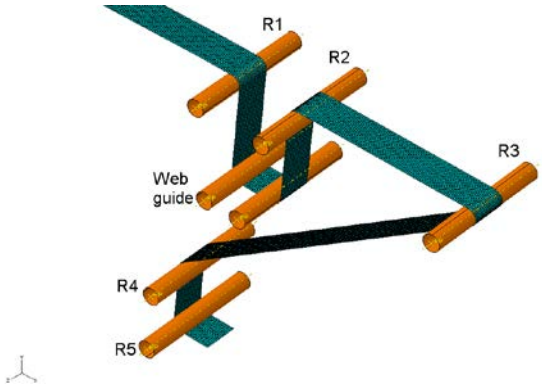

Figure 14 – Cambered web model setup

The importance of entering slope has been stated in last sections. But what will happen if the entering slope to test span could be controlled, such as, normal entry to the test span? To conduct this, a different model as shown in Figure 14 is used to run the simulations with zero entering slopes to the test span. The model shown in Figure 14 has a 762 mm span before the test span which is between R3 and R4. In this case, web guide

tries to steer the camber out at entry of R2 and the normal entry is achieved at the entry to R3, which has been proved in previous sections. Therefore, the cambered web enters the test span with zero slope. In the simulations using this model, two different friction coefficient combinations are employed. A friction coefficient is set as 0.3 on every roller in the low friction coefficient study. To study high friction coefficient effect, rough contact is used only on R4 and 0.3 is used for rest rollers. Rough contact is an option supplied by Abaqus which means the friction coefficient is infinite and there is no slippage happens during contact. The simulation time is 80 seconds because of additional span between R2 and R3. The shell element S4R is used as well.

Low Friction Study

Figure 15 shows the deformed coordinate along centerline of web when it enters different rollers from two applied tension cases which are 17.8 N and 53.4 N, and slopes are shown in the figures as well. Entry and exit positions of rollers R2, R3 and R4 are shown as vertical lines. All the curves are acquired from 80 seconds of simulations. Figure 16 shows deformed coordinate at centerline of web through time at the entries of to R2, R3 and R4, and exit of R2 for different tensions. The entry to R2 is where the web guide starts to steer the camber and makes the web enter R2 with a deformed coordinate near zero. In two plots in Figure 15, the deformed coordinates at entry and exit of R2 are all very close to zero. It can be seen in Figure 16 the deformed coordinates at entry and exit of R2 in two cases are all small through the simulation time.

The calculated slopes of the lateral deformed coordinate on R2 are not zero. Swanson reported slopes at the exit of R2 that were non-zero as well [3]. The web guide controls the lateral position of the web but it does not control the slope. This behavior would exist for real web guides too as those which are simulated herein. This issue is somewhat more complex for a cambered web whose slope varies with the MD position in the camber. Note from Figures 15 (a) & (b) that the web transits R2 at some non-zero slope and then enters and crosses R3 at a slope very close to zero. As mentioned previously, the entering slope to the test span is critical in determining if a cambered web steers. With the 762 mm span between R2 and R3, normal entry can be achieved at the entry to R3 for the applied tensions and friction level.

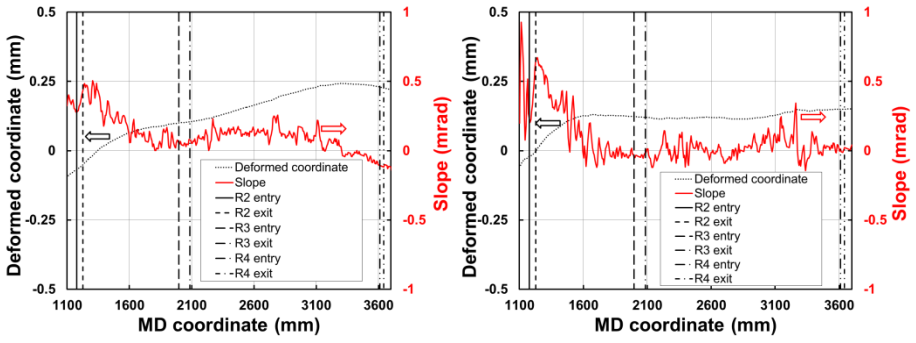

Figure 15 – Lateral (CMD) deformed coordinate along MD direction: (a) 17.8 N tension and friction coefficient is 0.3 on all rollers; (b) 53.4 N tension and friction coefficient is 0.3 on all rollers.

As shown in Table 3, the relative displacements are in small magnitude (0.025 mm). Meanwhile, the curves in Figure 15 show have higher noise levels. Thus it is necessary to prove the decrease in relative displacement is numerically significant instead of only noises. The lateral displacement and calculated slope from a simulation which has a straight web running through four aligned rollers is conducted to prove this. The lateral displacement of the web moving on aligned rollers is in the magnitude of 2.5×10^{-4} mm, which is negligible compared to the ones shown in Figure 16. The decline of relative displacement with increasing tensions shown in Table 3 is not merely numerical noisy effect.

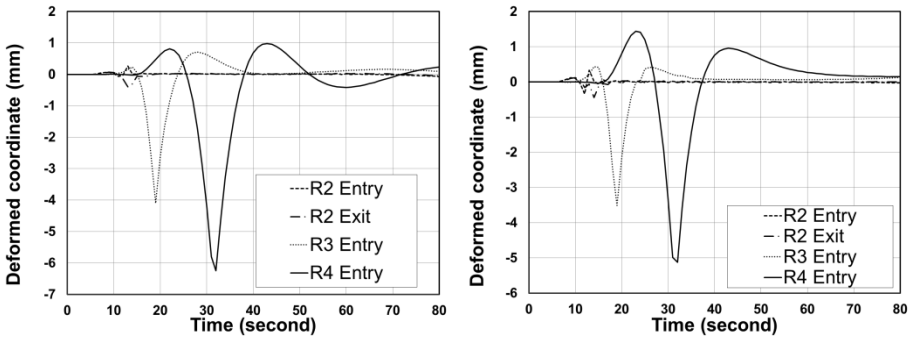

(a) (b)

Figure 16 – Lateral deformed coordinate against time: (a) 17.8 N tension and friction coefficient is 0.3 on all rollers; (b) 53.4 N tension and friction coefficient is 0.3 on all rollers.

Figure 15 shows when the web entering R3 at normal entry in all cases because the slope curve approaches zero at the entry of R3. Furthermore, the web is steered to the longer side or low tension side, which agrees qualitatively with the experimental results [1] and [3]. In Figure 16, it could be seen that R3 Entry curves oscillate at the beginning of the simulations when the cambered web enters the R2-R3 span. The cambered web is defined in a free span prior to rollers in the initial state and the downstream web that wraps the rollers is straight, in this case, when the cambered web moves into spans it will induce dynamic behavior. This is why the curves oscillate dramatically at the beginning of simulations.

In the test span, the web response is only controlled by applied tension and friction forces generated on the rollers. Normal entry is also achieved when the web reaches entry to R4 at high tension case. The R4 Entry curve in Figure 15 (a) shows the web is approaching the normal entry at the end of the simulation, but more time is required to fully converge. The combination of low friction coefficient, the longer effective span length (R2-R3 plus R3-R4 spans) and low tension, required additional computational time to reach a steady state solution. Unlike Figure 15 (a), R4 Entry curves in Figure 15 (b) have reached steady status before the end of simulations. The simulation data in Table 3 and in Figures 15 and 16 do show a slight decline in relative displacement between R3 and R4. For a low friction coefficient 3M test results show little relative displacement in Table 3. The test results show steering (in the magnitude of 10^{-2} mm) with inconsistency in sign. It might be argued the steering was essentially zero at all tensions because the test results are comparable to the accuracy by which a web can be slit with a stationary knife.

The simulation results and test results are in same magnitude, but they do not agree with each other well. The calculated slopes using the polynomials defined by output from 5 edge sensors do indicate the cambered web enters test span with a nonzero slope [3]. However, the entering slope to test span is close zero since normal entry has been achieved using 2nd model. Essentially, this case does not have same boundary conditions as experiments have.

As mentioned in previous sections, the theoretical moment to straighten the camber is 0.447 N·m. This value is shown in Figure 17, and it is close to calculated moment. The moment curves appear to have some tension dependency as well: The lowest tension produces a descending moment curve in test span and the average value is 0.434 N·m lower than 0.447 N·m. The 53.4 N curve has less oscillation and is much closer to a straight line, and the average value 0.450 N·m which is close to 0.446 N·m as well. Therefore, the moment calculated using elementary beam theory is very close to the moment generated in cambered web when it travels through rollers in simulations using 2nd model.

Applied tensions (N)	Simulation			Test results (mm)
	Deformed coordinate at R3 Entry (mm)	Deformed coordinate at R4 Entry (mm)	Relative displacement (mm)	
17.8	0.099	0.231	0.132	-0.028
53.4	0.122	0.150	0.028	0.028

Table 3 Simulations vs. Experiments

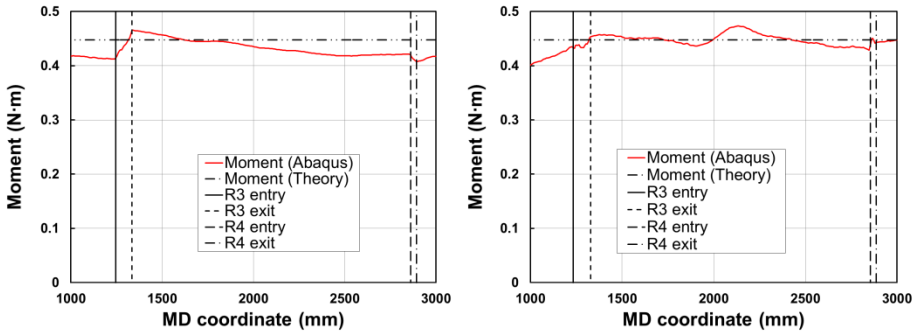

Figure 17 – Calculated moments along MD direction: (a) 17.8 N tension and friction coefficient is 0.3 on all rollers; (b) 53.4 N tension and friction coefficient is 0.3 on all rollers.

High Friction Study

Additional simulations are conducted using the 2nd model with the exception of a high friction (rough) coefficient of contact assigned on R4 are discussed in this section. Two different tensions, 17.8 N and 53.4 N are applied in the simulations. Similar to Figures 15 and 16, Figure 18 shows the deformed lateral coordinate at the center line of the web as it enters different rollers, and slopes from two cases are shown in same plot.

Figure 19 shows the deformed coordinate of the center line of the web through time at the entries to R2, R3 and R4, and exit of R2 from two different cases.

In both cases, web enters R3 normally which is same as what shown in Figure 15. In the low tension case shown as Figure 18 (a), the web also enters R4 normally caused by high friction contact on R4. At same the tension level (17.8 N) shown in Figure 15 (a) with low friction contact did not result in steady state by the end of simulation. The web is steered towards to the longer side in the 17.8 N case, and the relative displacement is almost zero for 53.4 N case. These agree with the results in low friction cases.

Applied tensions (N)	Simulation			Test results (mm)
	Deformed coordinate at R3 Entry (mm)	Deformed coordinate at R4 Entry (mm)	Relative displacement (mm)	
17.8	0.102	0.243	0.142	1.473
53.4	0.124	0.097	-0.028	0.064

Table 4 – Simulations vs. Experiments

However, simulation results do not indicate similar friction coefficient effect as experiments. The relative displacements from two simulations are shown in Table 4. The simulation results and test results do not match with each other. But as mentioned previously in this section, the entry slope to test span is close to zero due to the web attaining normal entry to R3 in these simulations, hence the boundary conditions are different in simulations which induce different lateral movement. The intention of simulations using 2nd model is to explore the effect of zero entering slope instead of comparing to the test results. From the simulation results, zero entering slope induces zero downstream steering no matter what friction coefficient applied.

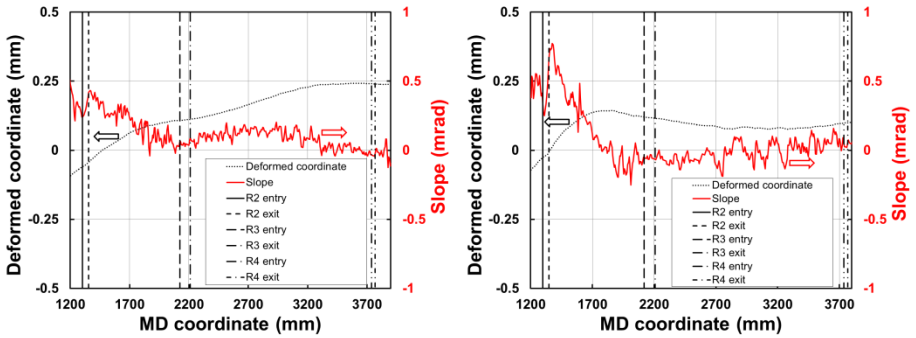

(a) (b)

Figure 18 – Lateral deformed coordinate along MD direction: (a) 17.8 N tension and friction coefficient is 0.3 on all rollers except R4 which is rough contact; (b) 53.4 N tension and friction coefficient is 0.3 on all rollers except R4 which is rough contact.

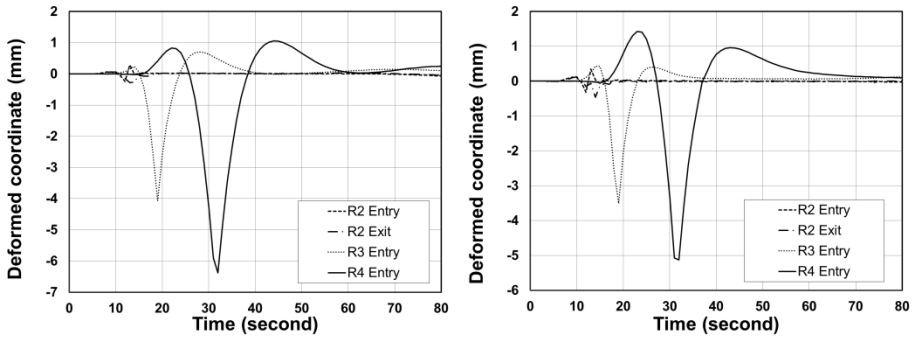

(a) (b)

Figure 19 – Lateral deformed coordinate against time: (a) 17.8 N tension and friction coefficient is 0.3 on all rollers except R4 which is rough contact; (b) 53.4 N tension and friction coefficient is 0.3 on all rollers except R4 which is rough contact.

Moments are calculated using MD stresses are shown in Figure 20. The theoretical moment using Bernoulli-Euler equation, 0.447 N·m, is shown as horizontal line. High friction contact on R4 affects moment response more in the low tension case than the high tension case. Compared to Figure 17 (a), the moment curve in Figure 20 (a) is closer to theoretical calculation, and the average value is 0.44 N·m.

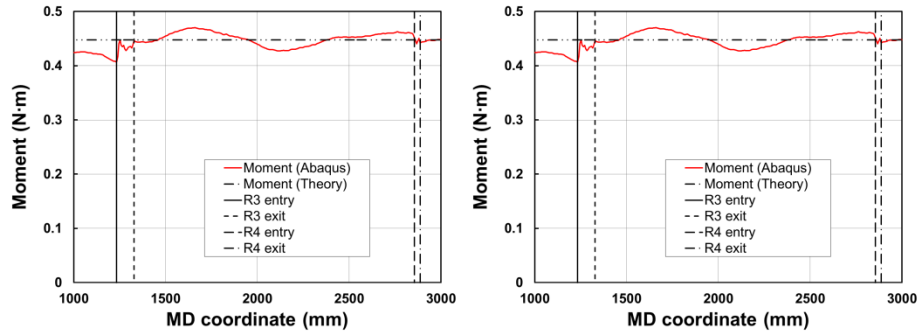

(a) (b)

Figure 20 – Calculated moment along MD direction: (a) 17.8 N tension and friction coefficient is 0.3 on all rollers except R4 which is rough contact; (b) 53.4 N tension and friction coefficient is 0.3 on all rollers except R4 which is rough contact.

DISCUSSIONS

Two different models are employed in this study: using the 1st model, a nonzero slope is generated as web entering test span; there is no slope generated when the web enters test span in the 2nd model. The deformed CMD coordinates from simulation outputs have been studied. The tendency of cambered web response has been compared to the conclusions made based upon experimental results. In the 17.8 N cases using the 1st model, there is an entering slope, about 1.25 mrads, consistently generated for 0.3 friction coefficient on every roller case. With a nonzero entering slope to enter test span, the

steering of web at downstream end is about 0.762 mm. The entering slope is caused by combination effect of camber of web, applied tension and web guide rotation. The simulation results do not show any friction coefficient dependency. In the 2nd model, deformed coordinates of centerline of cambered web and corresponding calculated slope show that the web enters R3 and test span normally, which means entering slope is close to zero. The low tension and low coefficient cause web to reach steady state on R4 in a longer time; on the other hand, high friction coefficient contact can result in achieving normal entry on R4 in a shorter time. The amount of steering is relatively small in all the 2nd model simulations, and there is almost no steering of web and the relative deformed coordinates are close to zero in the high tension case. In all the simulations, cambered web steers towards to the low tension (longer) side web, which agrees with previous experimental results reported in [1]-[3].

In previous publications, the debate and argument on the 4th boundary condition, moment or curvature, have been lasting for years. But there is no commanding conclusion has been made yet. Additionally, other boundary conditions have not been concluded either, as Swanson [3] suggests: the 2nd boundary, the slope of web at entry to test span, in cambered web analysis needs more study. The major focus of this simulation work is to explore the boundary conditions of cambered web moving through a series of rollers instead of exactly matching experimental results. The reason why it is not realistic to model exact experimental set-up in the simulations, thus comparable results to tests from simulations may not be necessary. In fact, by adjusting model setup, simulation results could agree with experimental results. However, this kind of adjustment is not meaningful. The effect of boundary conditions on web response is more important if the simulations can provide reliable results for different conditions.

Even in the tests, different measurement conditions lead to inconsistent results and conclusions: in [2], Swanson reported test results on cambered web steering, however, these results do not agree with the measurements conducted later in [3], even the conclusions on effect of steering are different. But this does not mean either of them is incorrect, because the measurement data taken during tests was limited. There are nothing but upstream and downstream lateral positions were measured and reported in [3]. The slopes reported in the same paper were calculated using displacement data instead of be measured directly. There is no information on slopes shown in [1] and [2] either.

Thus the tendency of cambered web response and boundary condition effects should be studied more to make conclusions instead of simply matching the deformed coordinates from simulations with recorded experimental results. Simulations with friction coefficient 0.3 and 17.8 N tension using two different models are analyzed at first. In the 1st model, about 0.762 mm relatively lateral movement is achieved in the simulations under same frictional condition, which is caused by a nonzero upstream slope (1.25 mrads) in test span. On the other hand, the 762 mm span between R2 and R3 in the 2nd model results in a normal entry (zero entering slope) to test span, which induces really tiny steering value, about -0.132 mm. This leads to the first conclusion of this study: the upstream slope in test span significantly affects downstream steering of cambered web in test span, which means a smaller upstream slope induces less downstream steering.

The upstream slope could be affected by several different factors, such as, camber in the web, friction coefficient on upstream roller, length of test span and web guide rotation. The 2nd conclusion could be drawn from high and low tension level simulations using different model setups. Simulations conducted using both models all indicate the relationship between applied tension and lateral movement: lateral movement decreases with applied tension increased, which agrees with experimental observation. Essentially, same conclusion was made in [1] and [3] based upon their experimental results as well.

In addition, different friction coefficient combinations using two models were also examined. Three different friction coefficient values were used on R3, 0.1, 0.3 and 4.0 in the cases using 1st model. Two different friction coefficients are used on R4, 0.3 and rough in the cases using 2nd model. The results do not vary with friction coefficient changing on R3 (1st model) or R4 (2nd model). However, the experimental results and conclusions reported in [3] do show the friction coefficient dependency on downstream roller of test span. It might be argued that the experimental conditions result in the friction coefficient dependency or the models used in this simulation work induce different working condition with tests.

To study the 4th boundary conditions, the moments are calculated using MD stresses. Calculated moments using results from 2nd model show a constant value and are very close to the moment calculated using equation {1}. The 1st model shows that moments increase almost linearly from upstream to downstream in test span and the moment approaches theoretical value at downstream end (R3 entry). Figure 8 illustrates the moments are smaller than theoretical calculation at different tensions. It appears that the moment relates to the slope at the exit of upstream roller: a nearly zero slope induces almost constant moment in test span, which is shown in Figures 16 and 20; on the other hand, nonzero slope results in a nearly linearly increasing moment curve shown in Figures 6 and 10. The moment is also affected by applied tension: lower tension leads to larger off-set from theoretical calculation. In addition, the low tension simulations using 2nd model indicates moment curve is closer to theoretical calculation when the high friction contact on downstream roller (R4) is applied.

CONCLUSIONS

An automatic self-controlled web guide has been successfully modeled using Abaqus/Explicit for the first time with user defined subroutine VUAMP, which leads to possible simulations of cambered web moving through a series of rollers. This is a combination of finite element method and control theory. Cambered web is steered to the low tension side which agrees with previously reported experimental results. Cambered web enters downstream roller in test span normally as expected. The 2nd boundary condition, the entering slope to test span, was proven critical for cambered web steering. Zero entering slope results in only small downstream steering. A nonzero upstream slope induces downstream steering is verified in the simulations. The nonzero entering slope is caused by the camber and affected by applied tension.

Abaqus simulations have shown that the internal moment in the web is equal to the theoretical moment (EI/ρ) that would be required to cause the cambered web to become straight at the downstream end of the web span. Thus the 4th boundary condition for the cambered web could be that it enters the downstream roller with finite moment but zero curvature. This is similar but not equivalent to Shelton's 4th boundary condition for a straight web entering a misaligned roller [11]. Shelton stated that the moment in the straight web at the entry to a mislaigned downstream roller was zero. For the straight web this is equivalent to stating that the curvature of the web entering the misaligned roller is zero. Perhaps the 4th boundary condition is that the web is entering the downstream roller with zero curvature, regardless whether the case is a straight web entering a misaligned roller or a cambered web entering an aligned roller. Dependency on friction coefficient effect could not be verified using the two models in these simulations. Consequently, the entering slope is the only dominating factor found on the steering.

ACKNOWLEDGEMENTS

The authors would like to thank the industrial sponsors of Web Handling Research Center at Oklahoma State University for providing the funding which made this study possible. The test results shown in this work were acquired at the Corporate Research Labs of 3M Company.

REFERENCE

1. Shelton, J. J., "Effects of Web Camber of Handling," Proceedings of the Fourth International Conference on Web Handling, June 1997, Oklahoma State University.
2. Swanson, R. P., "Mechanics of Non-uniform Webs," Proceedings of the Fifth International Conference on Web Handling, June 1999, Oklahoma State University.
3. Swanson, R. P., "Lateral Dynamics of Non-uniform Webs," Proceedings of the Eleventh International Conference on Web Handling, June 2009, Oklahoma State University.
4. Benson, R. C., "Lateral Dynamics of a Moving Web with Geometrical Imperfection," Journal of Dynamic Systems, Measurement, and Control, Vol. 124, March 2002, pp. 25-34.
5. Jones, D. P., "Web Sag and the Effect of Camber on Steering." Proceedings of the Ninth International Conference on Web Handling, June 2007, Oklahoma State University.
6. Olsen, J. E., "Lateral Mechanics of An Imperfect Web," Proceedings of the Sixth International Conference on Web Handling, June 2001, Oklahoma State University.
7. Olsen, J. E., "Shear Effect and Lateral Dynamics of Imperfect Webs," Proceedings of the Seventh International Conference on Web Handling, June 2003, Oklahoma State University.
8. Olsen, J. E., "Lateral Mechanics of Baggy Webs at Low Tensions," Proceedings of the Eighth International Conference on Web Handling, June 2005, Oklahoma State University.
9. Olsen, J. E., "An Updated Model for Lateral Displacement of Non-uniform Webs," Proceedings of the Tenth International Conference on Web Handling, June 2009, Oklahoma State University.
10. Abaqus Documentation/Abaqus Analysis User's Manual, 2012.
11. Shelton, J.J., "Lateral Dynamics of a Moving Web," PhD Thesis, Oklahoma State University, 1968, p.29.